

Design of Mobile Phone Lens with Extended Depth of Field Based on Point-spread Function Focus Invariance

Hsin-Yueh Sung^{*a}, Sidney S. Yang^a, Horng Chang^b

^aInstitute of Photonics Technologies, Department of Electric Engineering,
National Tsing Hua University, Hsinchu 300, Taiwan

^bIndustrial Technology Research Institute, Electronics and Opto-Electronics Research Lab.,
Hsinchu 310, Taiwan

ABSTRACT

Due to the application of mobile phone lens, the clear image for the different object distance from infinity to close-up creates a new bargaining. We found that wave-front coding applied to extend the depth of field may solve this problem. By means of using cubic phase mask (CPM), the blurred point-spread function (PSF) is substantially invariant to defocus. Thus, the ideal hyperfocal distance condition can be satisfied as long as the constant blurred image can eventually be recovered by a simple digital signal processing. In this paper, we propose a different design method of computational imaging lens for mobile phone up to ideal depth of field based on PSF focus invariance. Because of the difficulty for comparing the similarity to different PSFs, we define a new metric, of correlation, to evaluate and optimize the PSF similarity. Besides, by means of adding the anti-symmetric free form phase plate at aperture stop and using the correlation and Strehl ratio as the two major optimization operands, we can get the optimum phase plate surface to achieve the required extended depth of field (EDoF). The resulted PSF on focal plane is significantly invariant to object distance varying from infinity to 10cm.

Keywords: mobile phone lens, extended depth of field, wave-front coding, cubic phase mask, point-spread function, focus invariance, PSF similarity, Computational Imaging

1. INTRODUCTION

From the mobile phone lens application viewpoint, the clear image for different object distances from infinity to close-up is preferred [1-4]. Generally Speaking, the reasonable depth of field for mobile phone lens is about from 30cm to infinity.

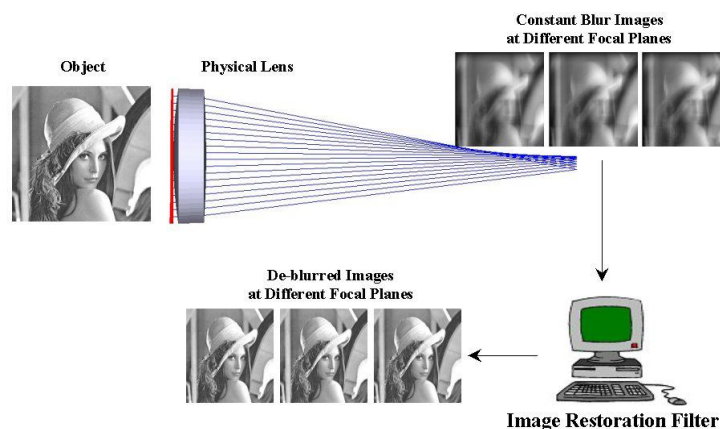


Fig.1. The Schematic Diagram for Focus Invariance.

*d938101@oz.nthu.edu.tw; phone 886-3-5731170; fax 886-3-5751113.

In other words, the hyperfocal distance is about 60cm. However, the required EDoF for market is of 10cm. In this EDoF condition, the focal length must less than 1.3mm while f-number is 2.8 in order to satisfied the quarter wavelength Rayleigh criterion. It is very difficult at the present time.

A novel technique, known as computational imaging, has been developed to increase the degrees of freedom or system trade space for designing a lens system. In traditional imaging, the concept of imaging relies on the design of lenses that rays diverging from a particular object point will intersect again at a corresponding point in a fixed image plane, then, constructing the image point by point. In computational imaging, the special phase surface are designed to alter or code the transmitted incoherent wave-front in such a way that the point-spread function (PSF) is not appreciably changed across a region near the focal plane. For examples, wave-front coding method [5-7] with the cubic phase mask (CPM) which has been proposed by Dowski and Cathey; the logarithmic asphere [8-9] which has been also proposed by George and Chi. Particularly, the wave-front coding method using CPM have been applied to many optical systems including infrared imaging systems by Dowski's Group [10] and Harvey's Group [11]. Because the PSF is significantly invariant to defocus, the post-processed image can be accurately decoded by a simple digital signal processing for an adequate range of defocus. The schematic diagram for focus invariance is shown in Fig.1.

In this paper, we propose a different approach for mobile phone lens design with the EDoF function based on PSF focus invariance. The PSFs of mobile phone lens are almost invariant to object distance change at fixed focal plane. In section 2 we describe the paraxial design for focus invariance requirement. The design method is presented in Section 3. The results are shown in Section 4. Section 5 concludes the paper.

2. PARAXIAL DESIGN FOR FOCUS INVARIANCE REQUIREMENT

Defocus aberration is caused simply by the dependence of the object distance change. In a traditional system the image distance can be defined by

$$\frac{1}{q} = \frac{1}{f} - \frac{1}{p} \quad (1)$$

For a fixed object distance p this system will focus at the same image distance q , give a fixed focal length f . However, the image distance is shift when the object distance changed. The difference of two image distances will produce misfocus. The amount of misfocus can be characterized by the defocus wave-front aberration W_{20} , which give by [12]

$$W_{20} = \frac{q_1 - q_2}{8(F/\#)^2} \quad (2)$$

where q_1 - q_2 is the difference of two image distances, and $F/\#$ is f-number. In general, the required EDoF specifications for mobile phone camera at present market are list in Table 1. In Fig.2 we show the defocus wave-front aberration W_{20} due to EDoF as a function of focal length according to the specifications in Table 1. As an example, a thin lens with focal length = 4mm, f-number = 2.8, and designed wavelength = 0.55 μ m, the image plane shift is approximately 166 μ m when the object distance varies from infinity to 10cm. The corresponding defocus wave-front aberration W_{20} is about $\pm 2.4\lambda$. This is just the required quantity for focus invariance with EDoF function. From a different viewpoint, in the same condition, when focal length is less than 1.3mm, the defocus wave-front aberration W_{20} satisfies the quarter wavelength Rayleigh criterion. In other words, the EDoF function is unnecessary if focal length is less than 1.3mm. As a result, the shorter the focal length, the smaller defocus aberration. It is easier to design the mobile phone lens with EDoF function when the induced defocus aberration is smaller.

Table 1. The EDoF Specifications for Mobile Phone Camera

Item	Value
Extended Depth of Field	10 cm ~ Infinity
F/Number	2.8
Designed Wavelength	0.55 μ m

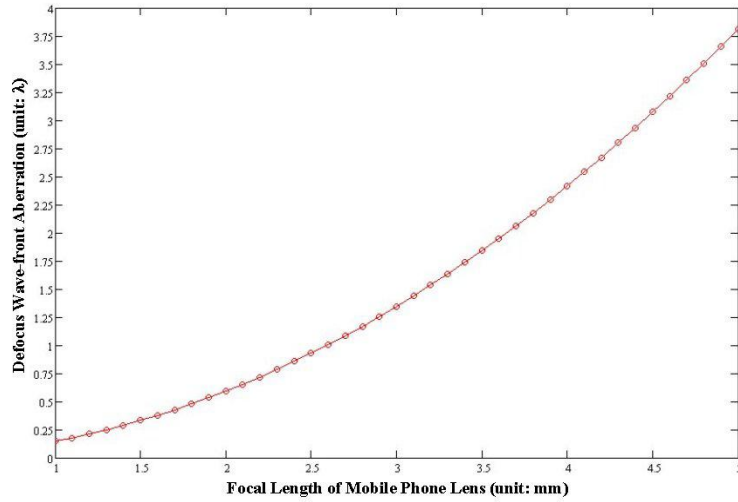


Fig.2. Defocus Wave-front Aberration due to EDoF as a Function of Focal Length

3. THE FOCUS INVARIANCE DESIGN USING PSF SIMILARITY

As is well-known, to manage the blurred PSF at different defocus, their forms have to be controlled not only with similarity but also compactness. The higher degree of similarity of these PSFs will provide simpler the image restoration scheme. Also, the smaller PSF size means the lower noise will be created after the digital signal processing. Due to the difficulty for comparing the similarity between two different PSFs, we define a new metric, of correlation [13], to quantify the PSF blur similarity. Thus, the correlation between the two PSFs as well as Strehl ratio optimizations are simultaneously used to control the PSF blur similarity and the PSF blur minimization respectively.

The steps of our investigation are as following:

Firstly, we design a typically traditional mobile phone lens as a starting case [14-17]. The object distance of the traditional mobile phone lens with the best performance is about 20cm. The specifications of the mobile phone lens are listed in Table 2. Fig.3 show the performance of traditional mobile phone lens at object distance 20cm, including (a) 2D lens layout, (b) modulation transfer function (MTF) curve, (c) ray aberration curve and (d) chief ray angle at image surface. Because the focal length of mobile phone lens is about 3.5mm, the required quantity for focus invariance is $W_{20} = \pm 1.84 \lambda$. The polychromatic PSF grey scale map at three different field positions and three different object distances are shown in Fig. 4. A single polychromatic PSF is computed according to a weighted combination of the monochromatic PSFs for each wavelength specified in the lens data. The corresponding wavelength weights are used weight these component PSFs. The result is a single-band polychromatic PSF. Obviously, when object distance changed from 20cm to 10cm or to infinity, it presents a very serious misfocus and the correspondent PSFs are changed enormously. This makes very difficult to remove the dissimilar blur spot with a simple digital filter. Fig. 4(b) and Fig. 4(c) show the differences for field 0.0. This demonstrates that, although the PSF size of traditional mobile phone lens is small enough at object distance 20cm, their performance cannot be maintained over a larger distance range of 10cm.

Next, an anti-symmetric free-form phase plate is added to the aperture stop. The anti-symmetric free-form phase plate is expressed as the classical polynomial expression

$$S(x, y) = \sum_{m=0}^{\infty} \sum_{n=0}^{\infty} C_{mn} x^m y^n, \quad m+n \leq 5 \quad \text{and} \quad m+n \in \text{odd number} \quad (3)$$

where C_{mn} are a set of coefficients that will be determined by optimization procedure described later. The main reason for using an anti-symmetric polynomial expansion in powers of x and y is for introducing rotationally asymmetric wave-

fronts like cubic phase mask. Thus, the anti-symmetric free-form surface must satisfy $S(-x,-y) = -S(x,y)$. Practically, we also constrain the highest order less five for polynomial expansion, i.e. $m + n \leq 5$.

Table 2. The Specifications for Traditional Mobile Phone Lens

Parameter	Value
Effective Focal Length	3.5 mm
F/Number	2.8
Design Wavelength	C, d ,F
FOV	±30°
Chief Ray Angle	< 22°
Optical Distortion	< 2%
TV Distortion	< 1%
Lateral Color	< 4μm
Relative Illumination	> 50%
Veiling Glare	< 7%
Total Track	< 5.4 mm
Lens Composition	2G2P ; [(+)-+]

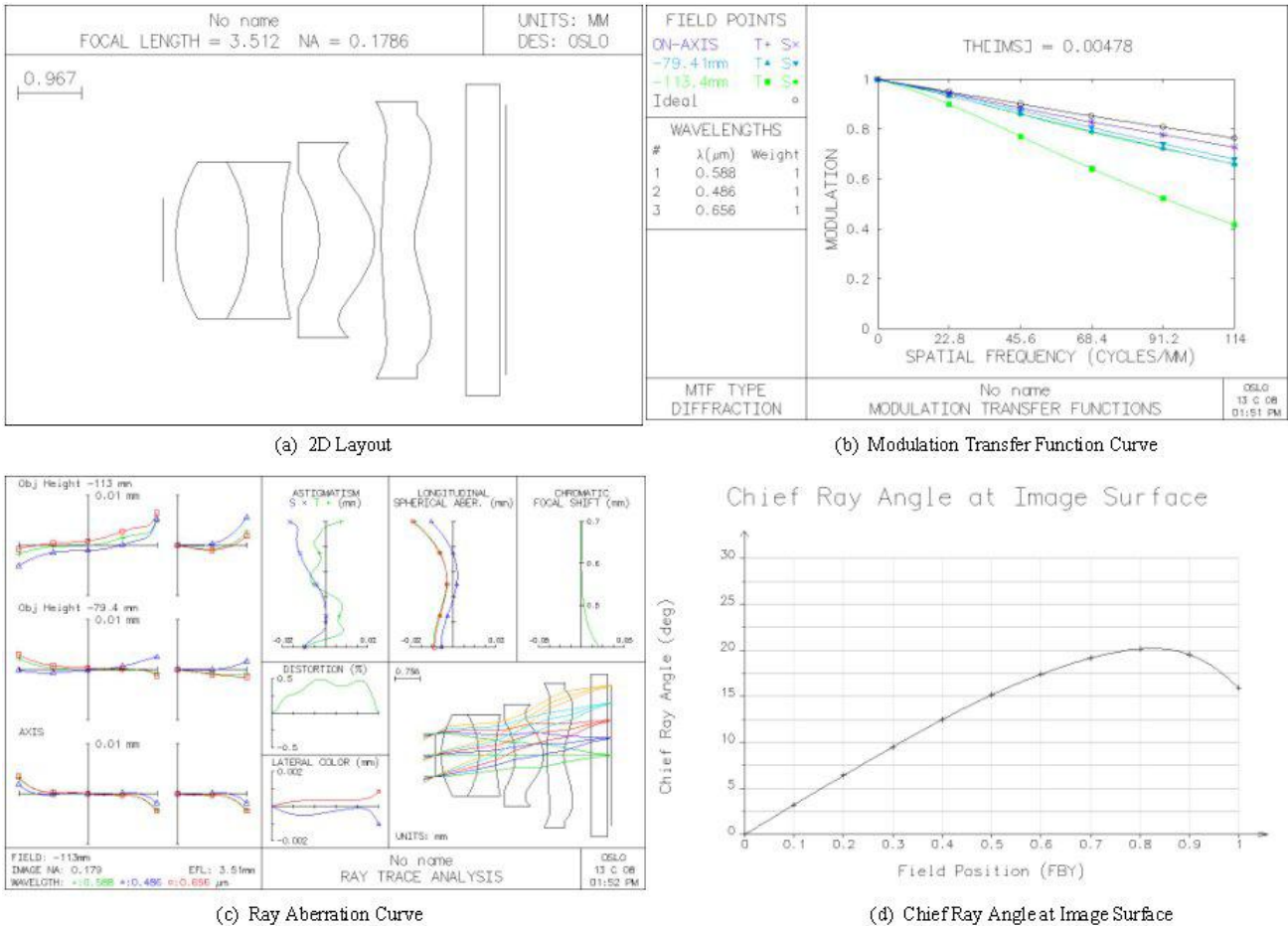
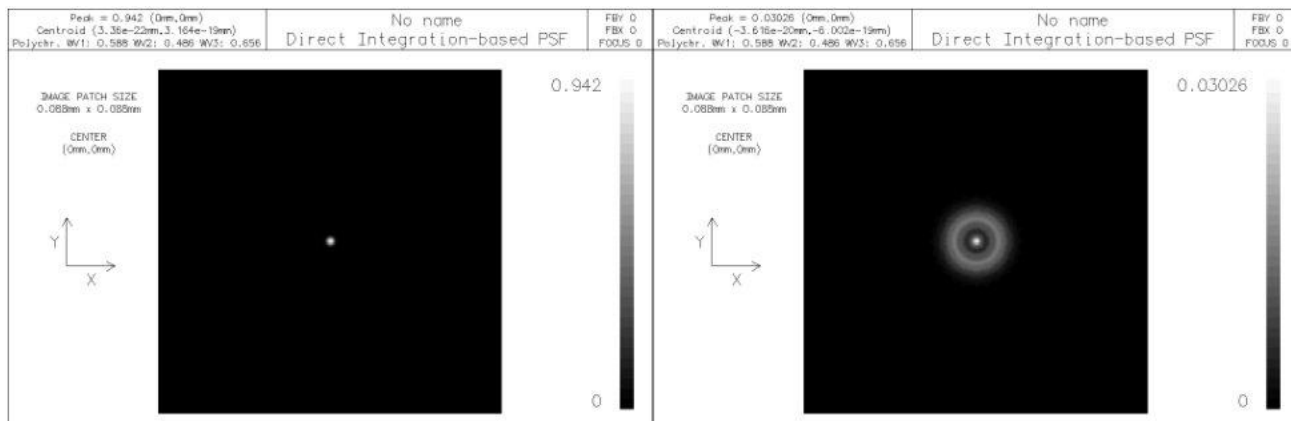


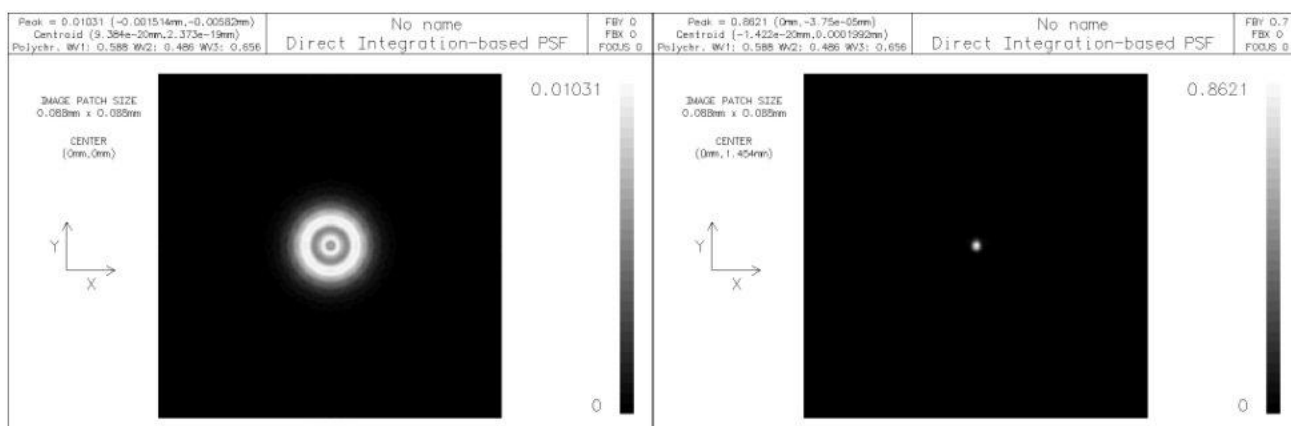
Fig.3. General Mobile Phone Lens Performance at Object Distance 20cm

(a) 2D Lens Layout, (b) MTF Curve, (c) Ray Aberration Curve, (d) Chief Ray Angle at Image Surface



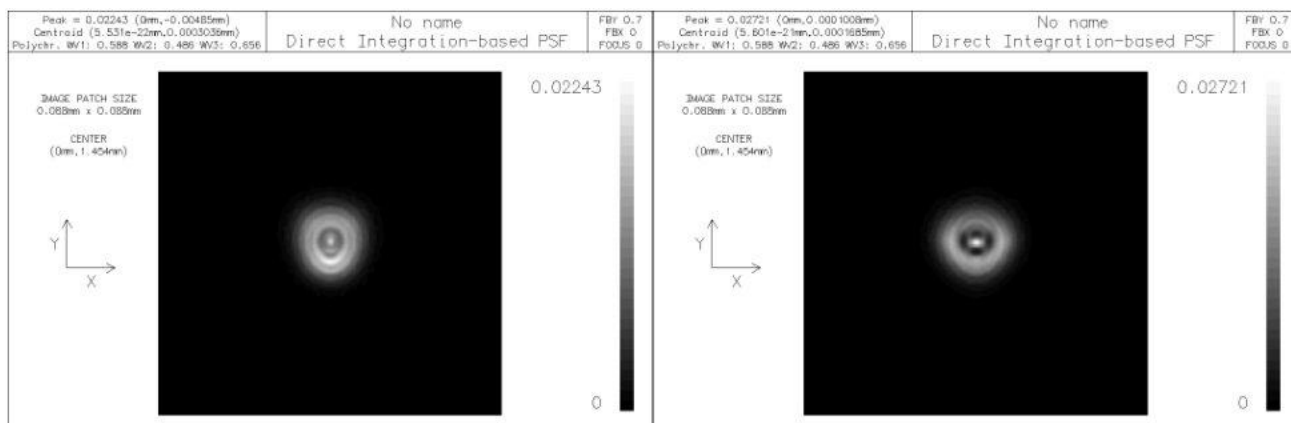
(a) PSF Gray Scale Map at Field 0.0 and Object Distance 20cm

(b) PSF Gray Scale Map at Field 0.0 and Object Distance 10cm



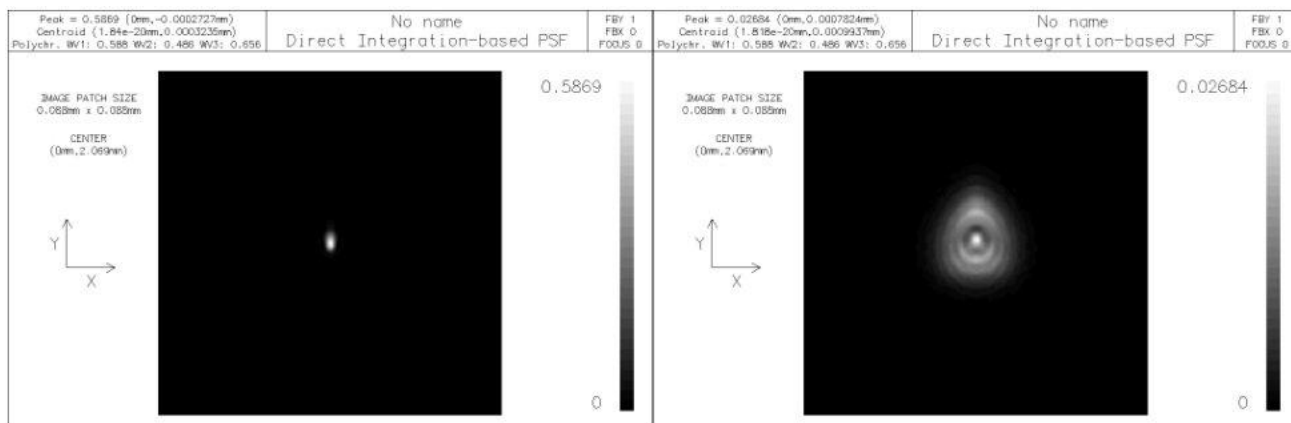
(c) PSF Gray Scale Map at Field 0.0 and Object Distance Infinity

(d) PSF Gray Scale Map at Field 0.7 and Object Distance 20cm



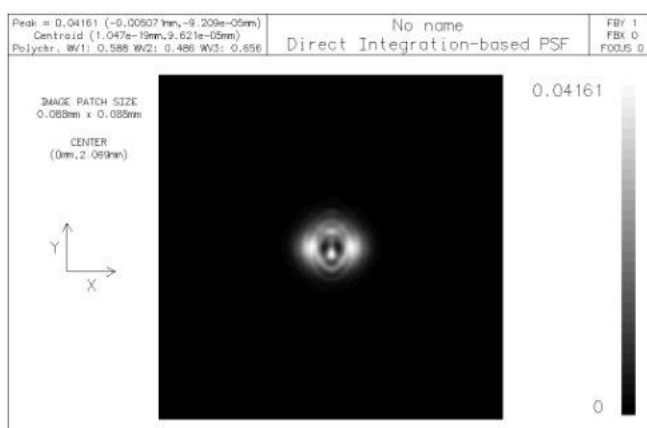
(e) PSF Gray Scale Map at Field 0.7 and Object Distance 10 cm

(f) PSF Gray Scale Map at Field 0.7 and Object Distance Infinity



(g) PSF Gray Scale Map at Field 1.0 and Object Distance 20 cm

(h) PSF Gray Scale Map at Field 1.0 and Object Distance 10 cm



(i) PSF Gray Scale Map at Field 1.0 and Object Distance Infinity

Fig.4. Polychromatic PSF Gray Scale Map for Traditional Mobile Phone Lens at Three Different Field Positions and Three Different Object Distances. (a) Field 0.0 and Object Distance 20cm, (b) Field 0.0 and Object Distance 10cm, (c) Field 0.0 and Object Distance Infinity, (d) Field 0.7 and Object Distance 20cm, (e) Field 0.7 and Object Distance 10cm, (f) Field 0.7 and Object Distance Infinity, (g) Field 1.0 and Object Distance 20cm, (h) Field 1.0 and Object Distance 10cm, (i) Field 1.0 and Object Distance Infinity.

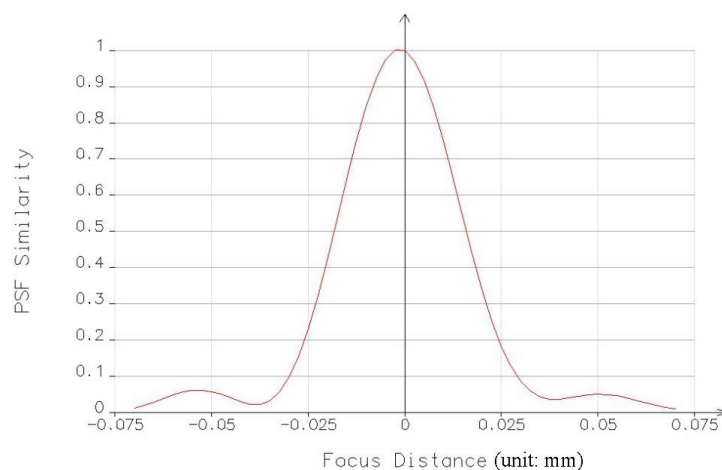


Fig.5. PSF Similarity Graph as a Function of Focal Distance Shift for Traditional Mobile Phone Lens at Field 0.0.

Thirdly, in order to design the EDoF mobile phone lens with the constant blurred PSF against object distance change, the correlation operand of two PSFs at different object distances and field positions are used for evaluating the PSF similarity. The definition of correlation is

$$C(PSF_R, PSF_T) = \frac{\int_{-\infty}^{\infty} \int_{-\infty}^{\infty} PSF_R(x, y) PSF_T(x, y) dx dy}{\int_{-\infty}^{\infty} \int_{-\infty}^{\infty} (PSF_R(x, y))^2 dx dy} \quad (4)$$

in which $PSF_R(x, y)$ is the reference PSF, $PSF_T(x, y)$ is the test PSF, and $C(PSF_R, PSF_T)$ is the PSF blur similarity for two different PSFs. In our case, the reference PSF is the PSF at Filed 0.0 and object distance 20cm. The test PSF is another PSF at some field position and object distance. Concurrently, in order to achieve the compact PSF, the Strehl Ratio operand is used to evaluate the PSF blur minimization. We construct the merit function by means of using the correlation and Strehl ratio as the two major optimization operands at three different field positions 0.0, 0.7, 1.0 and three different object distance 10cm, 20cm, infinity. In this paper, we adopt damped least square as optimization algorithm [18-19]. Thus, we can get the optimum phase plate surface form for PSF invariant against object distance change from infinity to 10cm and at all field of view. The optimized results are shown in Table 3.

Table 3. The anti-symmetric free-form surface and their coefficients C_{mn}

$S(x, y) = C_{05}y^5 + C_{23}x^2y^3 + C_{41}x^4y + C_{03}y^3 + C_{21}x^2y$				
C_{05}	C_{23}	C_{41}	C_{03}	C_{21}
0.01187	-0.02374	-0.07122	0.01257	-0.03771

4. THE PERFORMANCE AND COMPARISON

In this section, the performances of EDoF mobile phone lens with focus invariance are described. In order to compare these PSFs conveniently, the scale of each PSF map kept identically $88\mu\text{m}$ in Fig.4 and Fig.6. The polychromatic PSF gray scale maps for EDoF mobile phone lens at different object distance 20cm, 10cm, infinity and different field position 0.0, 0.7, 1.0 are shown in Fig.6. These PSFs are not only substantially similar but also significantly compact. As a comparison, the sizes of the PSFs in Fig.6 vary from $4.8\mu\text{m}$ to $7.5\mu\text{m}$, whereas the sizes of the PSFs in Fig.4 vary from $2\mu\text{m}$ to $22\mu\text{m}$.

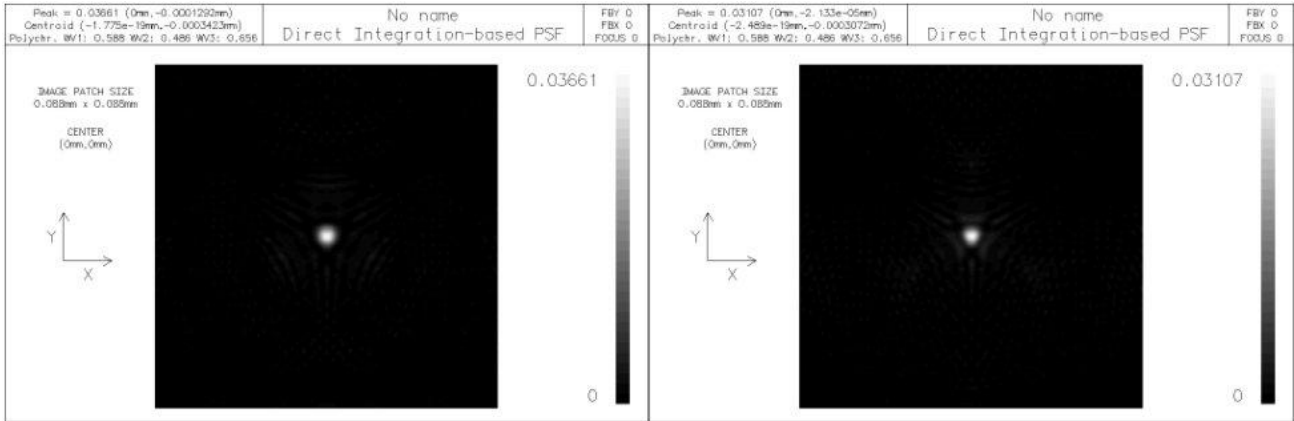
Additionally, Fig.5 and Fig.7 illustrate the PSF blur similarity graphs as a function of focal plane shift for traditional and EDoF mobile phone lens at Field 0.0. While the object distance varies from infinity to 10cm, the best image plane shift is about $\pm 0.064\text{mm}$. The PSF blur similarity graph in Fig.7 is better than that in Fig. 5. At object distance 10cm or infinity, the PSF similarity of EDoF mobile phone lens is an order of magnitude better than that of traditional mobile phone lens. We also demonstrate the simulated image results for traditional and EDoF mobile phone lens in Fig. 8 and Fig. 9. Because these PSFs at different object distance are substantially similar, a simple inverse restoration filter can be used to de-blur the blurred images at different object distance. In Fig. 9, it shows the de-blurred images at the different object distance are almost as same as original object image.

5. CONCLUSION

In this paper, a different approach to achieve the constant blur status of PSF at a certain defocused plane is proposed. The correlation between the two PSFs is adopted to control the PSF blur similarity, and concurrently, the Strehl ratio is also adopted to control the PSF blur minimization. The more similar between these PSFs, the simpler the restoration form needed. The smaller of these PSFs, the lower their noise be raised after post-processes. At object distance 10cm and infinity, the PSF similarity of EDoF mobile phone lens is an order of magnitude higher than that of traditional mobile phone lens. Because of the high PSF blur similarity at different object distance and field position, a simple inverse restoration filter can be used to de-blur the blurred images for an adequate range of object distance. Compared to the

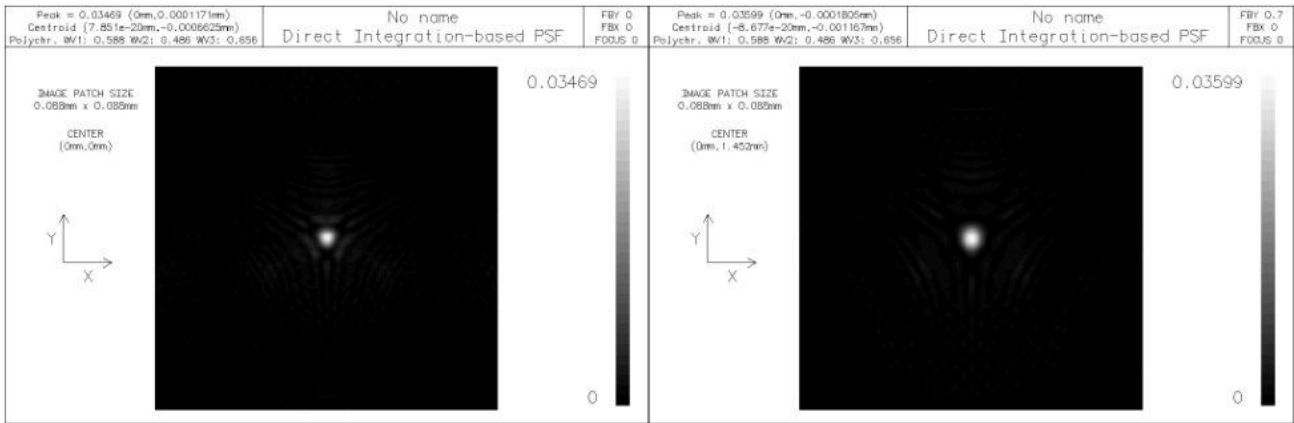
traditional mobile phone lens mentioned in introduction, the mobile phone lens with focus invariance is more large depth of field.

Acknowledgement: We thank Dr. Chang Chir-Weei in ITRI for the support of the project. We also thank Lambda Research Corp. for the educational support of simulation package, OSLO.



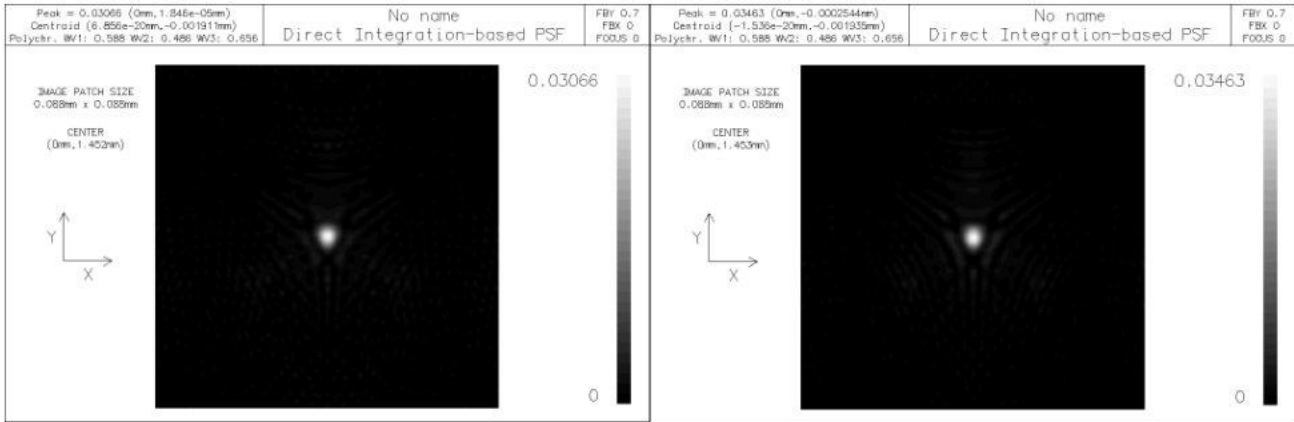
(a) PSF Gray Scale Map at Field 0.0 and Object Distance 20cm

(b) PSF Gray Scale Map at Field 0.0 and Object Distance 10cm



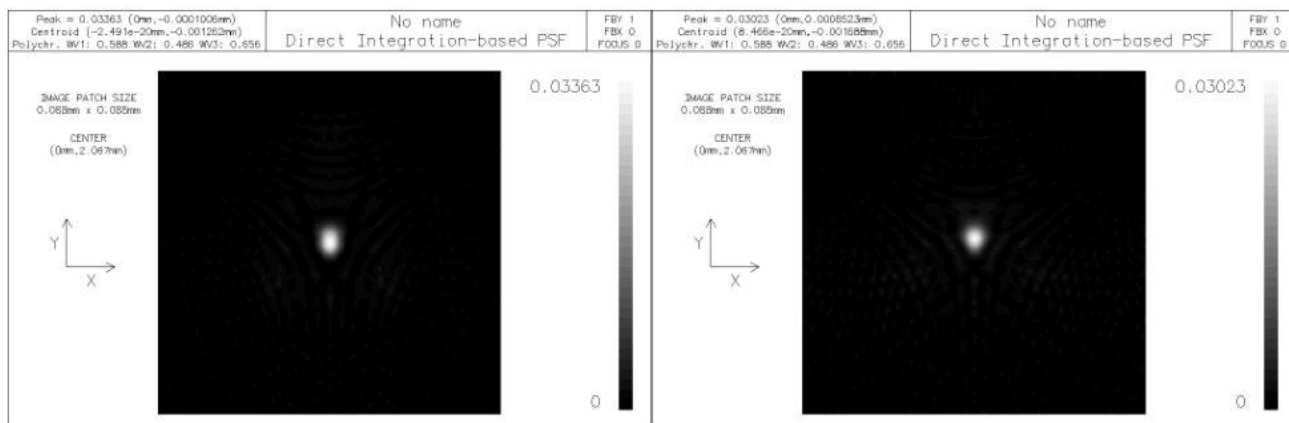
(c) PSF Gray Scale Map at Field 0.0 and Object Distance Infinity

(d) PSF Gray Scale Map at Field 0.7 and Object Distance 20cm



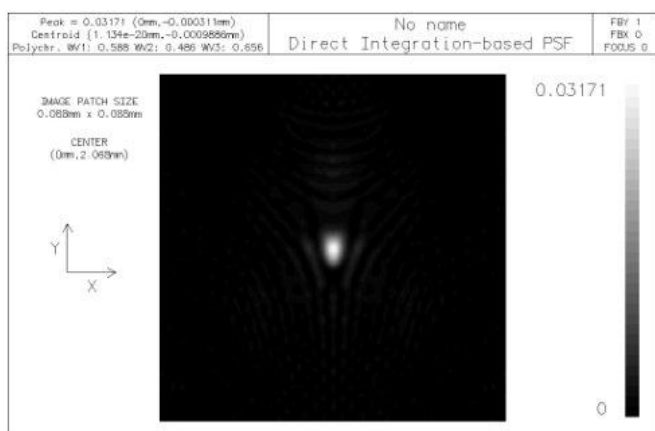
(e) PSF Gray Scale Map at Field 0.7 and Object Distance 10 cm

(f) PSF Gray Scale Map at Field 0.7 and Object Distance Infinity



(g) PSF Gray Scale Map at Field 1.0 and Object Distance 20 cm

(h) PSF Gray Scale Map at Field 1.0 and Object Distance 10 cm



(i) PSF Gray Scale Map at Field 1.0 and Object Distance Infinity

Fig.6. Polychromatic PSF Gray Scale Map for EDoF Mobile Phone Lens with Focus Invariance at Three Different Field Positions and Three Different Object Distances. (a) Field 0.0 and Object Distance 20cm, (b) Field 0.0 and Object Distance 10cm, (c) Field 0.0 and Object Distance Infinity, (d) Field 0.7 and Object Distance 20cm, (e) Field 0.7 and Object Distance 10cm, (f) Field 0.7 and Object Distance Infinity, (g) Field 1.0 and Object Distance 20cm, (h) Field 1.0 and Object Distance 10cm, (i) Field 1.0 and Object Distance Infinity.

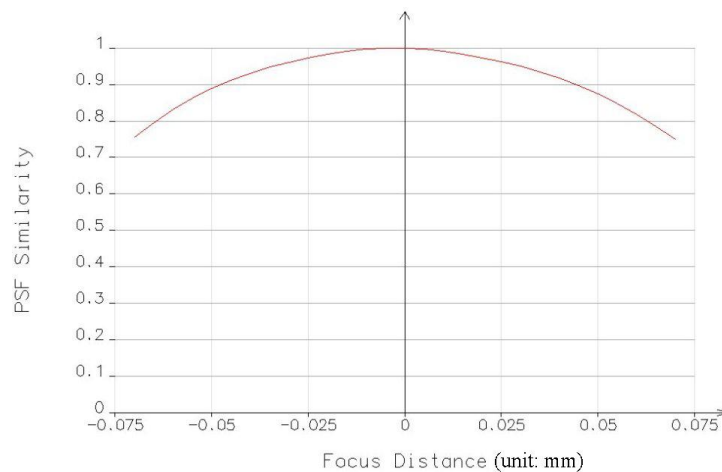


Fig.7. PSF Similarity Graph as a Function of Focal Distance Shift for EDoF Mobile Phone Lens at Field 0.0.

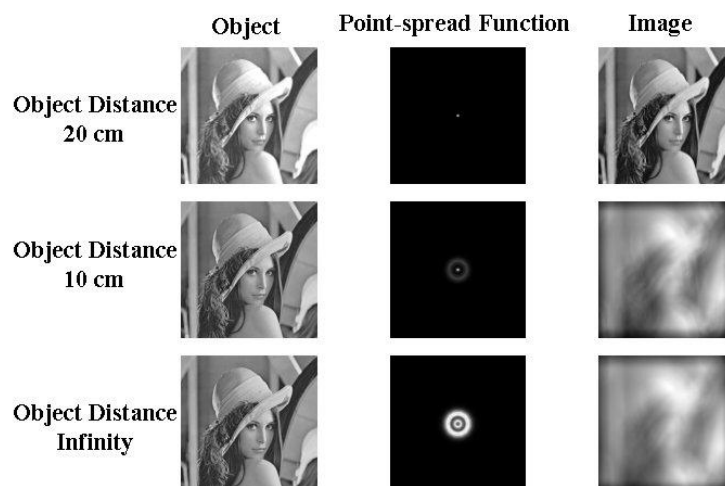


Fig.8. Simulated Images of Lena for Traditional Mobile Phone Lens at Different Object Distance and Field 0.0.

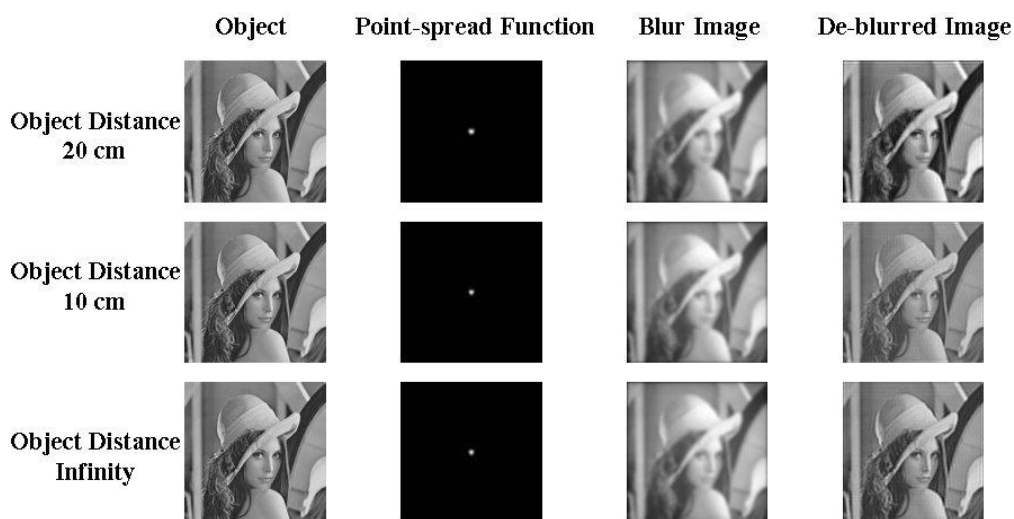


Fig.9. Simulated Images of Lena for EDoF Mobile Phone Lens at Different Object Distance and Field 0.0.

REFERENCES

1. J. Bareau and P. P. Clark, "The Optics of Miniature Digital Camera Modules", Proc. SPIE 6342, 63421F (2007).
2. V. Nummela, J. Viinikanoja, and J. Alakarhu, "Cameras in Mobile Phones", Proc. SPIE 6196, 61960B (2006).
3. E. Viger-Blanc, "Optics for Mobile Phone Imaging", Proc. SPIE 5249, 273-280 (2004).
4. S. Yamaguchi, H. Sato, N. Mori and T. Tiriki, "Recent technology and Usage of Plastic Lenses in Image Taking Objectives", Proc. SPIE 5872, 58720E (2004).
5. E. R. Dowski and W. T. Cathey, "Extended Depth of Field Through Wavefront Coding", Applied Optics, Vol. 34, No. 11, pp.1859-1866 (1995).
6. J. Gracht, E. R. Dowski, M. G. Taylor and D. Deaver, "Broadband Behavior of an Optical-digital Focus-invariant System", Optics Letters, Vol. 21, No.13, pp.919-921 (1996).
7. W. T. Cathey and E. R. Dowski, "New Paradigm for Imaging Systems", Applied Optics, Vol. 41, No. 29, pp.6080-6092 (2002).
8. W. Chi and N. George, "Electronic Imaging Using a Logarithmic Asphere", Optics Letters, Vol. 26, No. 12, pp. 875-877 (2001).
9. W. Chi and N. George, "Computational Imaging with the Logarithmic Asphere: Theory", J. Opt. Soc. Am. A Vol. 20, No. 12, pp. 2260- 2273 (2003).
10. E. R. Dowski, R. H. Cormack, and S. D. Sarama, "Wavefront Coding: Jointly Optimized Optical and Digital Imaging Systems", Proc. SPIE 4041 114-120 (2000).
11. G. Muyo and A. R. Harvey, "Wavefront Coding for Athermalization of Infrared Imaging Systems", Proc. SPIE 5612, 227-235 (2004).
12. R. E. Fischer, "Introduction to Optical System Design and Engineering", SPIE Short Course Notes (1992).
13. G. O. Reynolds, J. B. DeVelis, G. B. Parrent and B. J. Thompson: *The New Physical Optics Notebook Tutorials in Fourier Optics* (SPIE, Bellingham, 1989) pp.171-176
14. A. Ning, "Lens with External Aperture Stop", US Patent 6282033.
15. A. Ning, "Compact Lens with External Aperture Stop", US Patent 6441971.
16. C. S. Chen and Y. C. Huang, "Image Pickup Lens Assembly", US Patent 7355801.
17. S. Noda, "Four-Piece Lens Assembly", US Patent 7365920.
18. OSLO Optics Reference Version 6.1, Lambda Research Corporation (2001)
19. OSLO Program Reference Version 6.3, Lambda Research Corporation (2004)